Analysis of a special model for a grating coupler

W. L. Schaich
Department of Physics, Indiana University, Bloomington, Indiana 47405
(Received 14 January 2000)

A special model of a thin transmission grating used to couple infrared radiation to electronic excitations in quantum wells is examined. The grating is viewed as a periodic array of two-dimensional (2D) conducting strips separated by completely open apertures. The 2D conductivity across each strip has a semielliptic profile. This simple functional form allows considerable analytic progress. We examine both the recent approximation scheme proposed by Mikhailov for this class of grating and more complete theories. By physical arguments and numerical examples we show that Mikhailov's approximation can work very well, but that it is also rather easy to correct for its small errors.

I. INTRODUCTION

For the study of electronic excitations in quantum wells by infrared absorption one often uses an adjacent, planar grating to create field profiles that provide efficient coupling.[1,2] This wide experimental use of grating couplers has led to a variety of theoretical descriptions. In this paper we examine one particular class of models for which detailed calculations are possible. Since our interest here is in the behavior of the grating itself, we will usually consider these models in ''isolation''; i.e., the grating lies in the plane between vacuum and a homogeneous dielectric with nothing else nearby. The incident light enters along the normal from vacuum. We examine the currents in, the fields near, and the transmission through the grating.

The models we consider share some common features and approximations. The infrared wavelength, which is $\lambda = 1/\nu$ in vacuum, is assumed to be much greater than the period d of the grating, and the thickness of the grating is negligible. Thus the grating is viewed as a two-dimensional (2D) sheet whose conductivity is periodically modulated. With light incident along the normal and $\nu d < 1$, none of the diffracted waves can propagate away from the grating. They instead combine to form a complicated local field structure that is periodic parallel to the surface and decays exponentially away from it.

We assume the grating conductivity is local and isotropic, but it may be frequency dependent and complex valued. The grating lies on the y-z plane at $x=0$, between vacuum ($x<0$) and the substrate ($x>0$) with (bulk) dielectric constant ϵ_b. The axes are oriented so the 2D conductivity (conductance) σ is independent of z and periodic in y: $\sigma(y+d)=\sigma(y)$.[3] The particular class of models we consider is defined by the following form for the spatial modulation of σ (over one period):

$$\sigma(y)=\begin{cases}\sigma_{\max}\sqrt{1-\tilde{y}^2}, & |y|<w/2\\ 0, & w/2<|y|<d/2\end{cases} \tag{1}$$

where $\tilde{y}=2y/w$. The conducting stripes have width w and a ''semielliptic'' profile. They are separated by apertures of width $d-w$. This form for σ arises if each 2D conducting strip is viewed as the limit of an oblate spheroid with constant 3D conductivity that is distorted to large length along $\hat{z}$ and negligible thickness along $\hat{x}$. It also results from a strictly 2D model of any conducting strip for which the carriers are parabolically confined along $\hat{y}$.[4,5]

We concentrate on the case where the incident light has its electric field polarized along $\hat{y}$; i.e., orthogonal to the grating strips. The macroscopic quantity we calculate is the transmission coefficient, which can be parametrized by[3]

$$T=\left|\frac{2}{1+\sqrt{\epsilon_b}+(4\pi/c)\Sigma}\right|^2\sqrt{\epsilon_b}, \tag{2}$$

where c is the speed of light in vacuum and Σ is the y-y element of the effective conductance of the whole grating layer. To determine Σ requires a microscopic calculation.

The analysis is based on separating the total electric field into smooth and fluctuating parts:

$$\vec{E}=\vec{E}_s+\vec{E}_f. \tag{3}$$

The smooth part is described at frequency ω by

$$\vec{E}_s=E_{\rm inc}\hat{y}\times\begin{cases}e^{ip_v x}+r_o e^{-ip_v x}, & x<0\\ t_o e^{ip_b x}, & 0<x\end{cases} \tag{4}$$

where $E_{\rm inc}$ is the amplitude of the incident electric field and $p_v=\omega/c$ and $p_b=(\omega/c)\sqrt{\epsilon_b}$ are the wave vectors of the propagating solutions of Maxwell's equations in vacuum and bulk, respectively. The transmission and reflection amplitudes that appear here determine the transmission and reflection coefficients: $T=|t_0|^2\sqrt{\epsilon_b}$ and $R=|r_0|^2$. For the fluctuating field we use a variety of expressions, in all of which the speed of light is set to infinity, thereby suppressing retardation effects. This electrostatic approximation is reasonable as long as $\nu d \ll 1$.[3]

Before developing approaches to a solution of the model outlined above we remark that there are of course physical gratings and grating theories that do not use all of the simplifications proposed here.[1,2,6–15] However, the extensions and refinements they introduce are beyond the scope of this paper and we do not consider them in detail. Our simple treatment can be quite adequate for grating couplers of far-

infrared radiation and the particular conductivity profile of Eq. (1) allows considerable analytic progress.

In Sec. II we derive the equations behind several schemes for determining Σ. We start from the approximation introduced by Mikhailov.[16–20] Then by examining when and how it can fail, we develop better solutions. These formal results are evaluated in Sec. III in a set of model calculations. These are chosen to illustrate both the physical content and the numerical accuracy of the different approaches. Finally, in Sec. IV we discuss how the theories for an isolated grating can be generalized to include the effect of a nearby two-dimensional electron gas.

II. FORMAL SOLUTIONS

In this section we develop several approaches to solving our basic model.

A. Mikhailov's approximation

A remarkable feature of our model for the conducting strips is that any isolated strip when subjected to a uniform applied electric field along $\hat{y}$ responds so that the total electric field along $\hat{y}$ inside that strip is independent of position. This property is well known for 3D ellipsoids with constant conductivity.[21] We examine how it arises in 2D for a single strip because that will also show why it fails for an array of strips.

If a constant applied field does lead to a constant internal field, then the induced current would be of semielliptic form,

$$\hat{y}\cdot\vec{J}(y)=J(y)=\frac{4}{\pi}\overline{J}\sqrt{1-\tilde{y}^2},\quad |y|<w/2 \tag{5}$$

where $\overline{J}=(d/w)J_0$ is the current density (esu/cm sec) averaged over the width of the strip while J_0 is its average over one period of an array. From the equation of continuity, the induced charge density (esu/cm^2) in the strip would be

$$\delta\rho(y)=\frac{i}{\omega}\frac{8}{\pi}\frac{d}{w^2}J_0\frac{\tilde{y}}{\sqrt{1-\tilde{y}^2}},\quad |y|<w/2 \tag{6}$$

where the ω is the frequency of the applied field. Now use Eq. (6) in Coulomb's law to find the induced electric field along $\hat{y}$ at $x=0$:

$$\hat{y}\cdot\vec{E}_{\rm ind}(y)=E_{\parallel}(y)-E_0=\frac{2}{\kappa}\int\frac{dy'}{y-y'}\delta\rho(y'), \tag{7}$$

where $\kappa=(1+\epsilon_b)/2$ allows for the screening by the substrate dielectric and E_0 is the amplitude of the applied field. The integral yields[22]

$$E_{\parallel}(y)=E_0+\frac{i\tilde{J}_0}{\Gamma}\mathcal{E}_{\parallel}(y), \tag{8}$$

with

$$\mathcal{E}_{\parallel}(y)=\begin{cases}-1, & |y|<w/2\\ -1+\dfrac{\tilde{y}\,\mathrm{sgn}\,\tilde{y}}{\sqrt{\tilde{y}^2-1}}, & w/2<|y|.\end{cases} \tag{9}$$

Here $\tilde{J}_0=4\pi/cJ_0$ and the dimensionless parameter Γ is defined by

$$\Gamma=\frac{\pi^2}{4}\nu d(1+\epsilon_b)\frac{w^2}{d^2}, \tag{10}$$

with $\nu=\omega/2\pi c$. The electric field normal to the surface can also be readily found. We use the requirement that the discontinuity in the normal displacement field is determined by $\delta\rho$ in the grating plane. We shall refer to this constraint as the Poisson boundary condition. Here it implies near $x=0$

$$\hat{x}\cdot\vec{E}_{\rm ind}(y)=E_{\perp}(y)=i\frac{\tilde{J}_0}{\Gamma}\mathcal{E}_{\perp}(y)\mathrm{sgn}(x), \tag{11}$$

with

$$\mathcal{E}_{\perp}(y)=\begin{cases}\dfrac{\tilde{y}}{\sqrt{1-\tilde{y}^2}}, & |y|<w/2\\ 0, & w/2<|y|.\end{cases} \tag{12}$$

In order for our description to be consistent, $E_{\parallel}$ should be constant within the conducting strips. If only one strip is present, this is true by Eq. (9). However, for a grating we have a periodic array of strips and must use linear superposition. This is a trivial change for J, $\delta\rho$, and $E_{\perp}$ near $x=0$ since all of these quantities vanish away from the conducting strips. But when we rewrite $E_{\parallel}$ as

$$E_{\parallel}(y)=E_0+\frac{i\tilde{J}_0}{\Gamma}\sum_l\mathcal{E}_{\parallel}(y-ld), \tag{8'}$$

with l running over all integers, Eq. (9) then implies that the induced field is no longer constant across any strip. The decaying tails of the fields produced by neighboring strips extend into each strip, and the current distribution should change.

In Mikhailov's approximation[16–20] one ignores this inconsistency and assumes that the current density, even with a grating array, has a nearly semielliptic form. This physical ansatz is introduced as follows into a mathematical description based on Fourier series. In the electrostatic limit the full electric field near the (isolated) grating can be expanded for our models as[23]

$$\vec{E}(\vec{x})=E_0\hat{y}+\sum_{n>0}E_n(-\mathrm{sgn}(x)\sin G_n y,\cos G_n y,0)e^{-G_n|x|}, \tag{13}$$

where $G_n=2\pi n/d$ with n running over positive integers. The three components of the vectors in the sum are for the x,y,z directions, respectively. In reference to Eq. (4), what we have called the (smooth) applied field $E_0=E_{\rm inc}t_0=E_{\rm inc}(1+r_0)$, while the E_n for $n\neq 0$ describe the fluctuating

field. A similar expansion can be made for the current density in the plane of the grating

$$J(y)=J_0+\sum_{n>0} J_n \cos G_n y. \tag{14}$$

The terms in the series (13) already satisfy the boundary condition of continuous electric field parallel to the surface. Using the equation of continuity the Poisson boundary condition implies

$$F_n E_n=\tilde{J}_n, \tag{15}$$

with

$$F_n=i\nu d(1+\epsilon_b)/n. \tag{16}$$

Now write the spatially averaged current density as

$$J_0=\frac{1}{d}\int_{-d/2}^{d/2} dy\ \sigma(y)E_\parallel(y)=\sigma_0 E_0+\frac{1}{2}\sum_{n>0}\sigma_n E_n, \tag{17}$$

where the σ_n are (cosine) Fourier coefficients of $\sigma(y)$. For the semielliptic profile of Eq. (1),[24]

$$\tilde{\sigma}_n/\tilde{\sigma}_0=4\frac{J_1(G_n w/2)}{G_n w/2}\equiv\beta_n^{(1)}, \tag{18}$$

where J_1 is the Bessel function of order 1. Combining Eqs. (15) and (18) into (17) yields

$$\begin{aligned} J_0&=\sigma_0 E_0+\frac{\sigma_0}{2}\sum_{n>0}\frac{\beta_n^{(1)}\tilde{J}_n}{F_n}\\ &=\sigma_0 E_0\Big/\left(1-\frac{\tilde{\sigma}_0}{2}\sum_{n>0}\frac{\beta_n^{(1)}\tilde{J}_n/\tilde{J}_0}{F_n}\right). \end{aligned} \tag{19}$$

Equation (19) is exact but the $\tilde{J}_n$ are unknown. However if $J(y)$ is ''close'' to Eq. (5), one has $\tilde{J}_n/\tilde{J}_0\approx\beta_n^{(1)}$, which produces Mikhailov's approximation for $\Sigma\equiv J_0/E_0$:

$$\frac{4\pi}{c}\Sigma^{(M)}\approx\tilde{\sigma}_0/(1-A_{11}), \tag{20}$$

where

$$A_{11}=\frac{\tilde{\sigma}_0}{2}\sum_{n>0}\frac{\beta_n^{(1)}\beta_n^{(1)}}{F_n}=\frac{\tilde{\sigma}_0}{i\Gamma}\mathcal{A}_{11}. \tag{21}$$

It is not easy yet to estimate the error in this result. On the one hand, as $w/d\to 0$, it is clear that within any strip the tailing fields of its neighbors' contributions to $E_\parallel$ are small and slowly varying. Then the internal $E_\parallel$ is essentially constant. On the other hand, consider Mikhailov's prediction for large $\tilde{\sigma}_0$. Then

$$\frac{4\pi}{c}\Sigma^{(M)}\to\frac{-i\Gamma}{\mathcal{A}_{11}}. \tag{22}$$

If we further let $w\to d$ we expect Σ to diverge because one then has a continuous, perfectly conducting sheet. This does not happen with $\Sigma^{(M)}$ because Γ of Eq. (10) saturates and $\mathcal{A}_{11}$ decreases only to 0.285 at $w=d$. So the ansatz definitely fails in this extreme.

Before developing a better Σ, we briefly consider how to evaluate $\mathcal{A}_{11}$. A direct sum on n is possible, but converges slowly. The convergence problems are alleviated if one uses the Poisson summation formula to convert the sum on n to an integral and furthermore changes the contour for the integral:[16,17,19,25]

$$\begin{aligned} \mathcal{A}_{11}&=\frac{2\pi w}{d}\sum_{n>0}\frac{J_1^2(G_n w/2)}{G_n w/2}\\ &=2\int_0^\infty du\,\frac{J_1^2(u)}{u}\left[1+2\sum_{l>0}\cos u l\tilde{d}\right]\\ &=1-4\int_0^\infty dv\,\frac{I_1^2(v)}{v}\sum_{l>0}e^{-vl\tilde{d}}\\ &=1-4\int_0^\infty dv\,\frac{I_1^2(v)/v}{(e^{v\tilde{d}}-1)}, \end{aligned} \tag{23}$$

where $\tilde{d}=2d/w$ and I_1 is a modified Bessel function of order 1. The integral $\int_0^\infty du J_1^2(u)/u=1/2$ is from Ref. 26 and the integration contour was rotated by $\pm\pi/2$ between the second and third lines. Note that $\mathcal{A}_{11}$ is real-valued and depends only on the ratio w/d.

B. Density and potentials

For a more systematic approach to Σ, we next consider explicitly how a single strip responds to the electrostatic potentials produced by its neighbors. This analysis is straightforward for the case when the electrons in a grating strip are parabolically confined along $\hat{y}$ because the density response functions of this system are known ''exactly.''[5] We put exactly in quotes because the following expressions are derived in a ''classical continuum'' approximation that ignores pressure gradient forces and quantum size effects on the motion along $\hat{y}$.[4,5,27–29] This is reasonable for the systems of interest here since the Fermi wavelength of the electrons in the grating is much smaller than the strip width w ($\sim 1\ \mu$m).

The key function is the (self-) susceptibility $\chi^{(s)}$, which determines the (linearly) induced density in one strip due to an external potential $\phi^{\rm ext}$ at frequency ω:[5]

$$\delta\rho(y)=\int_{-w/2}^{w/2} dy'\chi^{(s)}(y,y')\varphi^{\rm ext}(y'), \tag{24}$$

where[30]

$$\chi^{(s)}(y,y')=\sum_j\left(\frac{2j}{\pi w}\frac{T_j(\tilde{y})}{\sqrt{1-\hat{y}^2}}\right)\frac{\kappa\Omega^2}{\tilde{\omega}^2-\omega_j^2}\left(\frac{2j}{\pi w}\frac{T_j(\tilde{y}')}{\sqrt{1-\tilde{y}'^2}}\right) \tag{25}$$

and the magnitude of y and y' must be less than $w/2$. The $T_j(\tilde{y})$ are Chebyshev polynomials of the first kind[26] and the sum index on j is over positive integers. The confining potential along $\hat{y}$ is described by $\frac{1}{2}m^*\Omega^2 y^2$ with m^* the effective electron mass. The frequencies of normal modes con-

fined along $\hat{y}$ but independent of z are $\omega_j=\sqrt{j}\Omega$. Finally $\tilde{\omega}^2=\omega(\omega+i/\tau)$, where $1/\tau$ parametrizes the strength of resistive scattering within the strip.

Consider first a single strip subjected to a uniform field along $\hat{y}$, so $\varphi^{\rm ext}(y)=-yE_0$. Then since $\tilde{y}=T_1(\tilde{y})$ and[31]

$$\int_{-1}^{1}\frac{d\tilde{y}}{\sqrt{1-\tilde{y}^2}}T_j(\tilde{y})T_k(\tilde{y})=\frac{\pi}{2}\delta_{j,k}, \tag{26}$$

we find from Eqs. (24) and (25)

$$\delta\rho^{(s)}(y)=-\frac{\kappa}{2\pi}\frac{\tilde{y}}{\sqrt{1-\tilde{y}^2}}E_0\frac{\Omega^2}{\tilde{\omega}^2-\Omega^2},\quad |y|<w/2. \tag{27}$$

Only the lowest frequency (Kohn) mode is dipole-allowed. This $\delta\rho^{(s)}$ has the same form as our earlier result (6), which may be rewritten as

$$\delta\rho^{(s)}(y)=-\frac{\kappa}{2\pi}\frac{\tilde{J}_0}{i\Gamma}\frac{\tilde{y}}{\sqrt{1-\tilde{y}^2}},\quad |y|<w/2. \tag{6'}$$

The superscript s is a reminder that the only electron-electron interactions allowed are within an isolated single strip. Equations (8) and (9) show that the internal field along $\hat{y}$ in an isolated single strip is $E_0-i\tilde{J}_0/\Gamma$ so

$$\tilde{J}_0=\tilde{\sigma}_0(E_0-i\tilde{J}_0/\Gamma)=\tilde{\sigma}_0E_0/(1-\tilde{\sigma}_0/i\Gamma). \tag{28}$$

Substituting this into Eq. (6′) we get complete agreement with Eq. (27) if

$$\tilde{\sigma}_0/i\Gamma=\Omega^2/\tilde{\omega}^2. \tag{29}$$

This result is consistent with the relation between the equilibrium density and the fundamental frequency.[5]

In a grating array of strips we must augment the external potential felt by any one strip. Since there is no variation along $\hat{z}$, the electrons interact like lines of charge with Coulomb coupling of the form

$$v(y,y')=-\frac{2}{\kappa}\ln|y-y'|. \tag{30}$$

Now formally separate v into $v^{(s)}+\delta v$ where for $v^{(s)}$ both y and y' lie in the same strip while for δv, y and y' must be in different strips. Then a mean-field argument yields for a periodic array in a uniform applied field

$$\delta\rho=\chi^{(s)}\cdot[-y'E_0+\delta v\cdot\delta\rho]=\delta\rho^{(s)}+\chi^{(s)}\cdot\delta v\cdot\delta\rho, \tag{31}$$

where we use centered dots for convolution integrals. This result implies that $\delta\rho$ can be expanded as

$$\delta\rho(y)=\sum_j c_j\frac{T_j(\tilde{y})}{\sqrt{1-\tilde{y}^2}},\quad |y|<w/2 \tag{32}$$

with only odd j's contributing to the sum. Combining the equation of continuity with another identity[31]

$$[T_j'(\tilde{y})\sqrt{1-\tilde{y}^2}]'=-j^2\frac{T_j(\tilde{y})}{\sqrt{1-\tilde{y}^2}}, \tag{33}$$

where primes denote $\tilde{y}$ derivatives, transforms Eq. (32) into an expansion of the current density

$$J(y)=-i\omega\frac{w}{2}\sum_j\frac{c_j}{j^2}T_j'(\tilde{y})\sqrt{1-\tilde{y}^2},\quad |y|<w/2. \tag{34}$$

To integrate this over the strip we use from Eq. (26)

$$\int_{-w/2}^{w/2}dy\,T_j'(\tilde{y})\sqrt{1-\tilde{y}^2}=\frac{\pi w}{4}\delta_{j,1} \tag{35}$$

to find

$$\tilde{J}_0=-\frac{2\pi i}{\kappa}\Gamma c_1. \tag{36}$$

Hence to determine $\tilde{J}_0$ we only need c_1, which, however, is coupled to the other c_j's through Eq. (31). A closed set of equations can be obtained by truncating the sum in Eq. (32) and then projecting Eq. (31) onto successive T_j.

To illustrate the method, let us keep only c_1 and c_3. They may be (approximately) determined from the projections of Eq. (31) onto T_1, using Eq. (26),

$$c_1=c_1^{(s)}+\frac{\kappa}{4}\frac{\Omega^2}{\tilde{\omega}^2-\Omega^2}[\delta v_{11}c_1+\delta v_{13}c_3], \tag{37}$$

and onto T_3

$$c_3=\frac{9\kappa}{4}\frac{\Omega^2}{\omega^2-3\Omega^2}[\delta v_{31}c_1+\delta v_{33}c_3], \tag{38}$$

where from Eq. (27) $c_1^{(s)}=-\kappa E_0/2\pi[\Omega^2/(\tilde{\omega}^2-\Omega^2)]$ and

$$\delta v_{jk}=\frac{2}{\pi}\int_{-1}^{1}d\tilde{y}\,\frac{2}{\pi}\int_{-1}^{1}d\tilde{y}'\frac{T_j(\tilde{y})}{\sqrt{1-\tilde{y}^2}}\delta\tilde{v}(y,y')\frac{T_k(\tilde{y}')}{\sqrt{1-\tilde{y}'^2}}. \tag{39}$$

The tilde on δv denotes a change in its meaning. We consider the interaction between electrons at y in one strip and electrons at $nd+y'$ in another strip, $n\neq 0$ periods away. Furthermore, we sum over all possible n and drop constant terms to define

$$\begin{aligned}\delta\tilde{v}(y,y')&=-\frac{2}{\kappa}\sum_{n>0}\ln\left[1-\left(\frac{y-y'}{nd}\right)^2\right]\\&\approx\frac{2}{\kappa}\sum_{n>0}\left\{\left(\frac{y-y'}{nd}\right)^2+\frac{1}{2}\left(\frac{y-y'}{nd}\right)^4+\cdots\right\},\end{aligned} \tag{40}$$

where the expansion in the second line is reasonable for $w\ll d$, since the maximum value of $|y-y'|$ is w. It is straightforward to work out the separate δv_{jk}. Expansions of y^l in terms of T_j for $j\leq l$ are in Ref. 31 and the sums of inverse powers of n become Riemann ζ functions, which also are in Ref. 31. We find that Eqs. (37) and (38) become

$$c_1 = c_1^{(s)} - \frac{\Omega^2}{\tilde{\omega}^2 - \Omega^2}\left\{\left(\frac{\pi w}{2d}\right)^2 \frac{1}{6}\left[1 + \frac{1}{10}\left(\frac{\pi w}{2d}\right)^2 + \dots\right] c_1 + \left(\frac{\pi w}{2d}\right)^4 \frac{1}{360} c_3\right\}, \tag{37'}$$

$$c_3 = 0 - \frac{9\Omega^2}{\tilde{\omega}^2 - 3\Omega^2}\left[\left(\frac{\pi w}{2d}\right)^4 \frac{1}{360} c_1 + \dots\right]. \tag{38'}$$

The ellipses denote terms missing because of the truncation in Eq. (40). Eliminate c_3 to solve for c_1 and use Eq. (36) to find $(4\pi/c)\Sigma = \tilde{J}_0/E_0$:

$$\frac{4\pi}{c}\Sigma \approx \frac{i\Gamma\Omega^2}{\tilde{\omega}^2 - \Omega^2\left\{1 - \left(\frac{\pi w}{2d}\right)^2 \frac{1}{6}\left[1 + \frac{1}{10}\left(\frac{\pi w}{2d}\right)^2 + \dots\right] + \frac{\Omega^2}{\tilde{\omega}^2 - 3\Omega^2}\left(\frac{\pi w}{2d}\right)^8 \left(\frac{1}{120}\right)^2 + \dots\right\}}. \tag{41}$$

Although the algebra is tedious, the final result for Σ is clear. There is a slight shift of the dipole resonance of a single strip to

$$\Omega^2\left\{1 - \left(\frac{\pi w}{2d}\right)^2 \frac{1}{6}\left[1 + \frac{1}{10}\left(\frac{\pi w}{2d}\right)^2 + \dots\right] - \frac{1}{2}\left(\frac{\pi w}{2d}\right)^8 \left(\frac{1}{120}\right)^2 + \dots\right\} \tag{42}$$

due to interactions between the strips and another (weak) resonance near $\sqrt{3}\Omega$. To compare with Mikhailov's approximation rewrite Eq. (20) using Eq. (29):

$$\frac{4\pi}{c}\Sigma^{(M)} \approx i\Gamma\Omega^2/(\tilde{\omega}^2 - \Omega^2\mathcal{A}_{11}). \tag{43}$$

His result follows in effect from keeping only the $j=1$ term in Eq. (32). For the dipole mode the amounts to a relative error of $o(w/d)^8$, which is very small for reasonable w/d values. The resonance at $\sqrt{3}\Omega$ is, however, completely missed, but its amplitude in Eq. (41) is also small. Equation (42) has noticeable differences with $\Omega^2\mathcal{A}_\parallel$ for $w/d \gtrsim 0.5$. These are mostly due to the expansion in Eq. (40). Mikhailov's approximation keeps only one term in Eq. (32), but all terms in Eq. (40). Including higher-order terms in Eq. (40) within the present approach is possible but clumsy. We turn instead to a slightly different approach that does not need such an expansion.

C. Current and fields

Our last approach to Σ is based on equating two different expansions of $E_\parallel(y)$. We first use $\tilde{J}(y) = \tilde{\sigma}(y)E_\parallel(y)$ combined with $\tilde{\sigma}(y) = (4/\pi)(d/w)\tilde{\sigma}_0\sqrt{1-\tilde{y}^2}$ inside a strip and Eqs. (34) and (36) to obtain

$$E_\parallel(y) = \frac{\tilde{J}_0}{\tilde{\sigma}_0}\sum_k \frac{c_k}{k^2 c_1} T_k', \quad |y| < w/2. \tag{44}$$

The alternative expansion comes from Eq. (13) at $x=0$:

$$E_\parallel(y) = E_0 + \sum_{n>0} E_n \cos G_n y. \tag{45}$$

We next equate Eqs. (44) and (45) and project onto $T_j'\sqrt{1-\tilde{y}^2}$ over $|y| < w/2$. One then needs two different sorts of integrals. The first is

$$\int_{-1}^{1} d\tilde{y}\sqrt{1-\tilde{y}^2}\,T_k' T_j' = \frac{\pi}{2} j^2 \delta_{k,j}, \tag{46}$$

which follows after an integration by parts from Eqs. (26) and (33). For the second set of integrals we define

$$\beta_n^{(j)} = \frac{4}{\pi}\int_{-1}^{1} d\tilde{y}\sqrt{1-\tilde{y}^2}\,T_j' \cos G_n y. \tag{47}$$

If j is an odd integer these may be transformed into[31]

$$\beta_n^{(j)} = 4j^2 i^{j-1}\frac{J_j(G_n w/2)}{G_n w/2}, \tag{48}$$

where J_j is a Bessel function of order j. Then Eqs. (44) and (45) together yield

$$\frac{c_j}{c_1} = \frac{\tilde{\sigma}_0 E_0}{\tilde{J}_0}\delta_{j,1} + \frac{\tilde{\sigma}_0}{2\tilde{J}_0}\sum_{n>0} E_n \beta_n^{(j)}. \tag{49}$$

Now replace E_n via Eq. (15) with $\tilde{J}_n/F_n$ and use from Eq. (34)

$$\tilde{J}_n = \frac{2}{d}\int_{-w/2}^{w/2} dy \cos G_n y\,\tilde{J}(y) = \tilde{J}_0 \sum_k \beta_n^{(k)}\frac{c_k}{k^2 c_1} \tag{50}$$

to re-express Eq. (49) as

$$\frac{c_j}{c_1} = \frac{\tilde{\sigma}_0 E_0}{\tilde{J}_0} + \sum_k A_{jk}\frac{c_k}{k^2 c_1}, \tag{51}$$

where

$$A_{jk} = \frac{\tilde{\sigma}_0}{2}\sum_{n>0}\frac{\beta_n^{(j)}\beta_n^{(k)}}{F_n} \equiv \frac{\tilde{\sigma}_0}{i\Gamma}\mathcal{A}_{jk}. \tag{52}$$

For $j=1$ this implies

$$\frac{4\pi}{c}\Sigma \equiv \tilde{J}_0/E_0 = \tilde{\sigma}_0 \Big/ \left(1-\sum_k A_{1k}\frac{c_k}{k^2 c_1}\right), \qquad (53)$$

which nicely generalizes Mikhailov's approximation (20). The c_k's for odd $k>1$ can be found by truncating the set of equations

$$\frac{c_j}{c_1} = A_{j1} + \sum_{k>1} A_{jk}\frac{c_k}{k^2 c_1}, \quad j>1. \qquad (54)$$

For numerical work the $\mathcal{A}_{jk}$ can be reduced as in Eq. (23):

$$\begin{aligned}\mathcal{A}_{jk} &= \frac{2\pi w}{d}\sum_{n>0} j^2 k^2 i^{j+k-2}\frac{J_j(G_n w/2)J_k(G_n w/2)}{G_n w/2} \\ &= 2j^2k^2 i^{j+k-2}\int_0^\infty du\,\frac{J_j(u)J_k(u)}{u}\left[1+2\sum_{l>0}\cos u l\tilde{d}\right] \\ &= j^3\delta_{j,k} - 4j^2k^2\int_0^\infty dv\frac{I_j(v)I_k(v)}{v}\sum_{l>0} e^{-vl\tilde{d}} \\ &= j^3\delta_{j,k} - 4j^2k^2\int_0^\infty dv\,\frac{I_j(v)I_k(v)/v}{(e^{v\tilde{d}}-1)}. \end{aligned} \qquad (55)$$

The integral used in the third line,

$$\int_0^\infty du\, J_j(u)J_k(u)/u = \frac{1}{2j}\delta_{j,k}, \qquad (56)$$

is from Ref. 32. Some insight is gained by separating $\mathcal{A}_{jk} = \mathcal{A}_{jk}^{(s)} + \delta\mathcal{A}_{jk}$, where $\mathcal{A}_{jk}^{(s)}$ is independent of d, while for small w/d, $\delta\mathcal{A}_{jk}\propto(w/d)^{j+k}$. One has for $j>1$ [using Eq. (29)]

$$\begin{aligned}&\left[\tilde{\omega}^2 - \Omega^2\left(j+\frac{\delta\mathcal{A}_{jj}}{j^2}\right)\right]\frac{c_j}{c_1} \\ &\qquad = \Omega^2\delta\mathcal{A}_{j1} + \Omega^2\sum_{\substack{k>1\\(k\neq j)}}\delta\mathcal{A}_{jk}\frac{c_k}{k^2c_1}, \end{aligned} \qquad (54')$$

which suggests that the higher c_j will be of small influence unless $w/d\to 1$ and/or the frequency ω is near one of the higher (dipole-forbidden) modes: $\omega_j=\sqrt{j}\Omega$. In turn if the higher c_j are unimportant, then Mikhailov's approximation should be good. To quantify these claims requires numerical work.

III. MODEL CALCULATIONS

In all the calculations below we use for the dielectric substrate $\epsilon_b=12.8$, which is appropriate for GaAs. The transmission into the bulk in the absence of any grating ($\Sigma=0$) is then $T=0.683$.

For the grating strips we first chose parameters so their intrinsic modes lie in the infrared. Mikhailov[20] describes the grating in this limit as quantum-well wires. We use an effective mass of $m^*/m=0.067$ and an average equilibrium density of $\overline{N}=3\times10^{11}/\mathrm{cm}^2$. The fundamental frequency determined by[4,5]

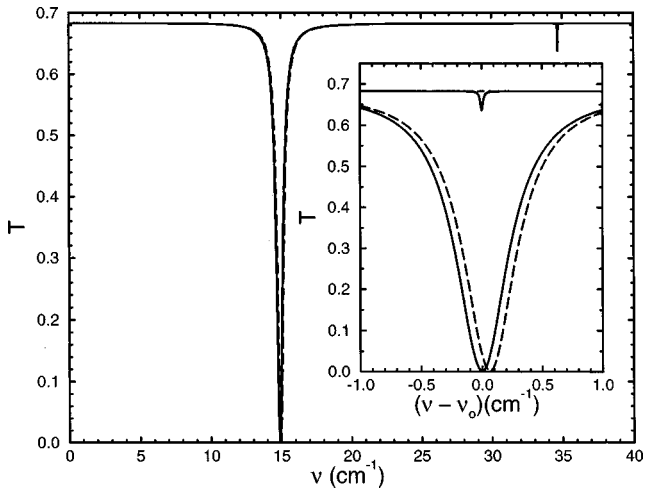

FIG. 1. Transmission T through an isolated grating versus frequency ν. The solid (dashed) curve is for the full (Mikhailov) Σ. The conducting strips of the grating have the response of quantum-well wires; see text for parameter choices. The insert expands the plot near the two sharp structures.

$$\Omega^2 = \frac{16}{\kappa}\frac{\overline{N}e^2}{m^* w} \qquad (57)$$

then has the value $\Omega/2\pi c=20.29\ \mathrm{cm}^{-1}$. We set $\tau=200$ ps, and $d=2\ \mu$m. In Fig. 1 the transmission coefficient over a range of frequencies near Ω is shown for the choice of $w/d=0.9$. Results are plotted for two different Σ expressions. One is from Eq. (57), cutting off the k sum at $k=9$, and the other is from Eq. (20), Mikhailov's approximation. We have chosen a large value of w/d in order to enhance the differences between the T's. Lowering w/d to 0.7 or less makes the two curves essentially lie on top of each other. The large structure centered on $\nu_0=14.88\ \mathrm{cm}^{-1}$ is due to the (significantly shifted) dipole-allowed mode, while the small dip at $\nu_0=34.68\ \mathrm{cm}^{-1}$ is from the excitation of the $j=3$ mode at nearly $\sqrt{3}\Omega$. The $j=5$ mode produces a blip at $45.3\ \mathrm{cm}^{-1}$, but it only changes T in the fourth digit.

The inset in Fig. 1 more clearly shows the two main structures. Mikhailov's approximation does quite well in the Kohn mode: it gives the correct depth and width and misses the resonance location by just 0.5%. The higher mode only shows up in the improved theory. Its strength and width are, however, quite small, basically because the mode is dipole-forbidden. For instance, its linewidth is set by $(2\pi c\tau)^{-1}=0.03\ \mathrm{cm}^{-1}$ with negligible contribution from radiation damping,[16–20] which dominates the width of the Kohn mode. The computational effort for the two sets of results is similar. One only needs a few more Bessel functions to evaluate Eq. (53). If I_1 is produced by a downward recursion,[33] the higher I_k are already generated.

We have also done a series of calculation of Σ's at fixed frequency ($\nu d=0.005$) when the grating strip conductance has metallic values, say $1/\overline{\sigma}=1\ \Omega/\square$. Again we compared various results for Σ. As a function of w/d, we find that the error in $\Sigma^{(M)}$ does not exceed 1% until $w/d>0.9$. As noted earlier Σ should diverge when $\omega\to d$, but $\Sigma^{(M)}$ saturates. The Σ from Eq. (53) does not appear to saturate. It is inter-

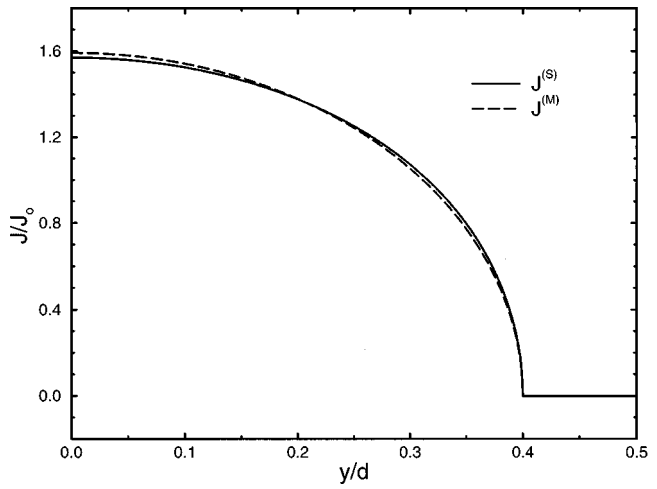

FIG. 2. Current density J in an isolated grating versus position y over half a period. The solid (dashed) curve is for the full (Mikhailov) theory. Only the real part of J/J_0 is shown. The average conductance of the grating strips is $\overline{\sigma}^{-1}=1\ \Omega/\square$ and $w/d=0.8$.

esting that its growth tracks closely the results for an array of perfectly conducting 2D strips. An expression for this idealized case can be found by a slight generalization of Lamb's century-old analysis.[34] The model has strips of width w and period d, across which the conductivity is constant (not semielliptic) and infinite. In our notation the resulting Σ is[35]

$$\frac{4\pi}{c}\Sigma^{(L)}=-i\frac{p_v d}{\pi}(1+\epsilon_b)\ln\sec\left(\frac{\pi}{2}\frac{w}{d}\right), \tag{58}$$

which has a ln divergence as $w/d\to 1$. We find that the imaginary part of Σ from Eq. (53) tracks this result fairly well for $\overline{\sigma}^{-1}\lesssim 1\ \Omega/\square$. (The real part of Σ is several orders of magnitude smaller.) For example at $\overline{\sigma}^{-1}=1\ \Omega/\square$ and $w/d=0.994$, $\mathrm{Im}(\Sigma)$ differs from $-i\Sigma^{(L)}$ by less than 1%, but differs from $\mathrm{Im}(\Sigma^{(M)})$ by more than 20%.

To provide some microscopic insight into the grating's behavior we show in Figs. 2–4 plots of current and fields in the grating plane. The calculations use $\nu d=0.005$, $\overline{\sigma}^{-1}=1\ \Omega/\square$, and $w/d=0.8$. For this case $\Sigma^{(M)}$ and the full Σ of (53) differ by about 0.1%. The quantities plotted come from either Sec. II A or Secs. II B and II C. For the former we use Eq. (5) for J, Eqs. (11) and (12) for $E_x(x=0^+)$, and Eqs. (8′) and (9) for E_y. For the latter we use from Eqs. (34) and (36)

$$J(y)/J_0=\frac{4}{\pi}\frac{d}{w}\left[1+\sum_{j>1}\frac{c_j}{j^2c_1}T_j'\right]\sqrt{1-\tilde{y}^2},\quad |y|<\frac{w}{2} \tag{59}$$

from Eq. (32) and the Poisson boundary condition

$$E_x(y)|_{x=0^+}=i\frac{\tilde{J}_0}{\Gamma}\left[\tilde{y}+\sum_{j>1}\frac{c_j}{j^2c_1}T_j\right]\Big/\sqrt{1-\tilde{y}^2},\quad |y|<\frac{w}{2} \tag{60}$$

and from Eq. (44)

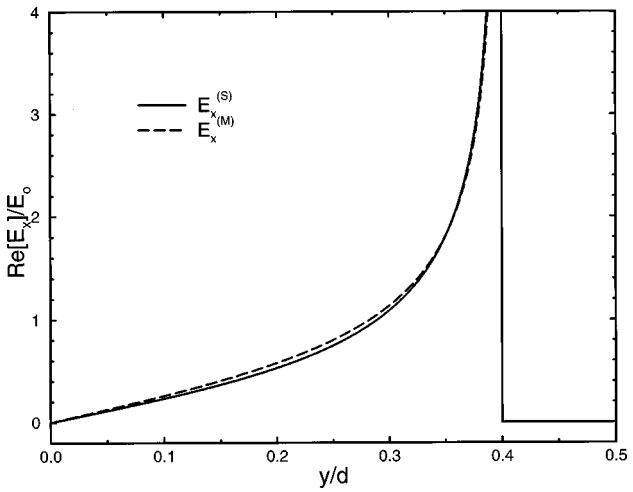

FIG. 3. Normal electric field E_x just above the plane of an isolated grating versus position y over half a period. The solid (dashed) curve is for the full (Mikhailov) theory. Only the real part of E_x/E_0 is shown. Parameters are the same as in Fig. 2.

$$E_y(y)=\frac{\tilde{J}_0}{\tilde{\sigma}_0}\left[1+\sum_{j>1}\frac{c_j}{j^2c_1}T_j'\right],\quad |y|<\frac{w}{2}. \tag{61}$$

In Figs. 2 and 3 the two sets of results are very similar. The current profile is nearly semielliptic and the changes in the charge distribution required by the full theory of Sec. II C are small. These behaviors arise numerically since the higher c_j's are small: $c_3/c_1\approx 0.045$, $c_5/c_1\approx 0.0059$, $c_7/c_1\approx 0.00075$, $c_9/c_1\approx 0.00010$, neglecting their much smaller imaginary parts.

In Fig. 4 significant differences appear. The two results being plotted differ roughly by a factor of $\Gamma/i\tilde{\sigma}_0$, which is imaginary. The disagreement is not evidence for a serious

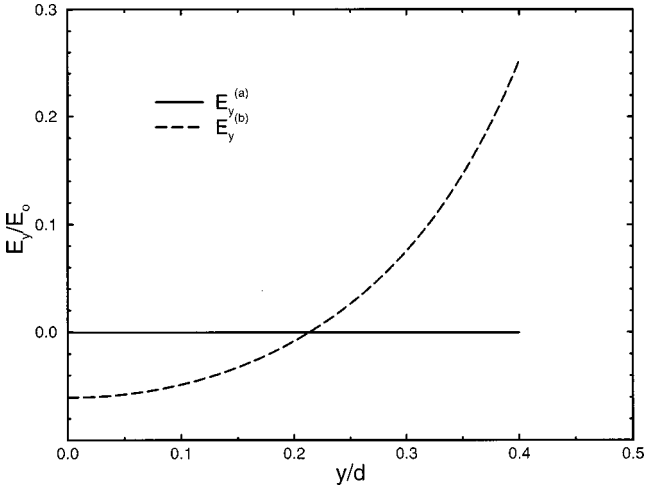

FIG. 4. Parallel electric field E_y in the plane of an isolated grating versus position y. The solid curve is the imaginary part of E_y for the full theory. Its value is within a few percent of $-0.000\,55$, while the real part is much smaller. The dashed curve is one version of the real part of E_y for Mikhailov's theory. Its imaginary part is much smaller. The spatial variation is due to the tails of the induced fields by neighboring strips. The parameters are the same as in Fig. 2 and we do not attempt to plot E_y outside the grating where it is much larger.

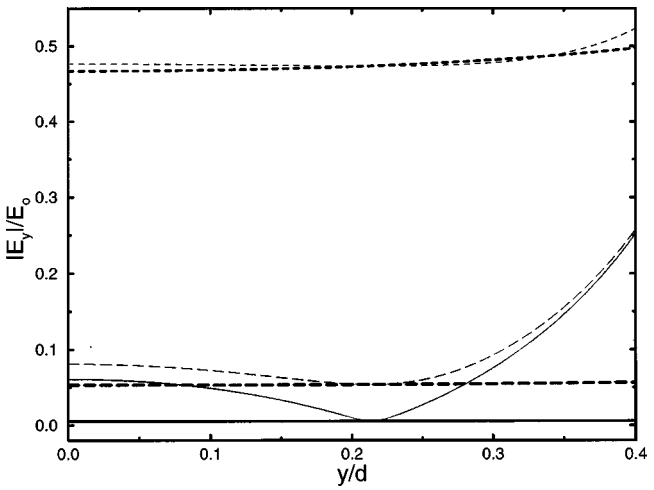

FIG. 5. Absolute magnitude of the parallel electric field E_y in the plane of an isolated grating versus position y. The thick (thin) curves are for the full (Mikhailov) theory. All parameters are the same as in Figs. 2–4 except the conductance $\bar{\sigma}$ whose inverse equals 10, 100, and 1000 $\Omega/\square$ for the solid, the long-dashed, and the short-dashed curves, respectively.

flaw in Mikhailov's approximation, but rather emphasizes how his scheme inconsistently treats $E_\parallel$. The quantity $E_y^{(b)}$ plotted in Fig. 4 is the field produced by currents that are *exactly* semielliptic. If one instead considers $J^{(M)}(y)/\sigma(y)$, one will instead have a small value that lies close to $E^{(a)}(y)$. This choice of two very distinct forms of E_y is the basic inconsistency in Mikhailov's approach. Although disconcerting in Fig. 4 it does not matter for $\Sigma^{(M)}$ of Eq. (20). A physical rationale for this seeming paradox is as follows. If one assumes a semi-elliptic form for $J(y)$, then an E_y profile such as that shown by $E^{(b)}(y)$ in Fig. 4 is produced within each strip. The electrons respond to this field, nearly screening it out. The amount of charge rearrangement needed for this screening is, however, rather small (see Fig. 3) and the profile of J remains close to semielliptic (see Fig. 2). One ends up with an internal $E_\parallel$ like that plotted as $E_y^{(a)}$ in Fig. 2.

This explanation invokes the notion of strong screening by a good conductor to resolve the difference between various E_y profiles in Mikhailov's approach. One might wonder if it breaks down if the grating strips become less conducting. In Fig. 5 we plot the absolute magnitude of E_y for several choices of $\bar{\sigma}$. This plotting scheme was chosen because the relative size of the real and imaginary parts of E_y depend on $\bar{\sigma}$. A significant qualitative change occurs when $\bar{\sigma}^{-1}$ jumps from 100 to 1000 $\Omega/\square$. For large values of $\bar{\sigma}$ strong screening occurs to bring the different E_y's into agreement, while for small values the various E_y's are initially nearly the same because so little screening is happening.[36] Remarkably Mikhailov's approximation for Σ gives three-digit accuracy for all the cases of Figs. 4 and 5).

Before ending this section we comment on the fact that we did not attempt to plot E_y past $y=w/2$. The basic reason is that we are avoiding numerical difficulties that do not matter for the calculation of Σ. Just outside each strip, $E_\parallel$ is divergent [see Eq. (9)] and we have not found a general and tractable expression for it, unlike $E_\perp$ in Eq. (60). We did try to use the Fourier series of Eq. (45), but a finite sum of terms cannot produce the singularity, whose influence slows the convergence for $y \approx w/2$. For the same reasons calculations based completely on Fourier series (with no T_j) do not converge well.[5,35] Similar convergence difficulties have been recently discussed for theories that use Fourier expansions[37] to determine the fields near gratings of non-negligible thickness.[38–43] Although these calculations examine a different geometrical parameter range (with λ comparable to both the period and thickness of the grating), they find analogous numerical difficulties. The cited authors have developed a variety of techniques to get around these problems.

IV. GENERALIZATIONS

Our aim here is to show that the schemes developed in Sec. II can still be applied when the grating is not isolated, but instead has a dynamic system nearby. We do this only for the simple, but widely practical, case in which the nearby system is homogenous in the y-z plane.[44] Then its response to the grating's fields can be described in terms of reflection amplitudes.

Start with a Fourier expansion of the electrostatic field. If the nearby system lies beyond $x=h$, one can write for $x<h$ as a generalization of Eq. (13)

$$\vec{E}(\vec{x}) = E_0\hat{y} + \sum_{n>0} E_n(-\mathrm{sgn}(x)\sin G_n y, \cos G_n y, 0)e^{-G_n|x|} + \sum_{n>0} e_n(\sin G_n y, \cos G_n y, 0)e^{-G_n(h-x)}. \tag{62}$$

Now view the e_n as arising from ''reflections'' of electrostatic waves off the system in $x>h$. Then using $\mathfrak{r}_n$ for the reflection amplitudes

$$e_n = \mathfrak{r}_n E_n e^{-G_n h}, \tag{63}$$

so $E_\parallel$ along $x=0$ can be written as

$$E_\parallel(y) = E_0 + \sum_{n>0} \mathcal{E}_n \cos G_n y, \tag{64}$$

where

$$\mathcal{E}_n = E_n(1+\mathfrak{r}_n e^{-2G_n h}). \tag{65}$$

Equations (64) and (65) generalize Eq. (45). Next combine Eqs. (14) and (62) with the Poisson boundary condition across $x=0$. The result has the same form as Eq. (15):

$$\mathcal{F}_n\mathcal{E}_n = \tilde{J}_n, \tag{15$'$}$$

where

$$\mathcal{F}_n = \frac{i\nu d}{n}\left(1+\epsilon_b - \frac{2\epsilon_b \mathfrak{r}_n e^{-2G_n h}}{1+\mathfrak{r}_n e^{-2G_n h}}\right). \tag{66}$$

We now have sufficient information to reproduce the approach to either Mikhailov's $\Sigma^{(M)}$ or the full Σ of Sec. II C, with the only change being that the A_{jk} of Eq. (52) are to be evaluated with the $\mathcal{F}_n$'s, rather than F_n's. Because of the exponential factor in Eq. (66), only the first few $\mathcal{F}_n$'s differ

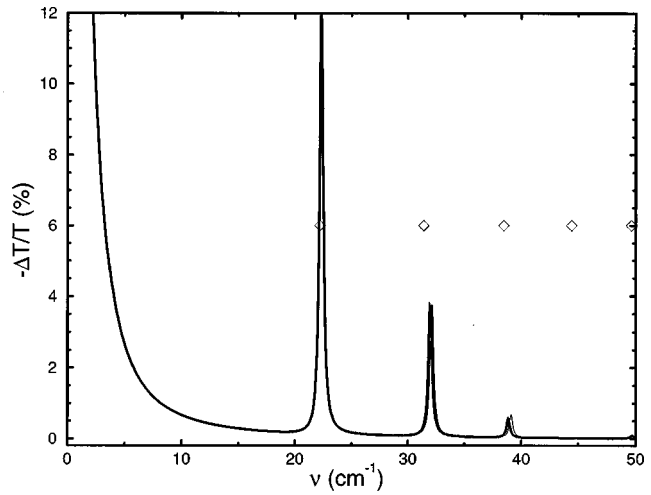

FIG. 6. Transmission spectrum of a grating and nearby 2DEG versus frequency ν. The solid (thin) curve is for the full (Mikhailov) treatment. The diamonds locate the modes of an unperturbed 2DEG; see Eq. (70). See text for parameter choices; $w/d=0.3$.

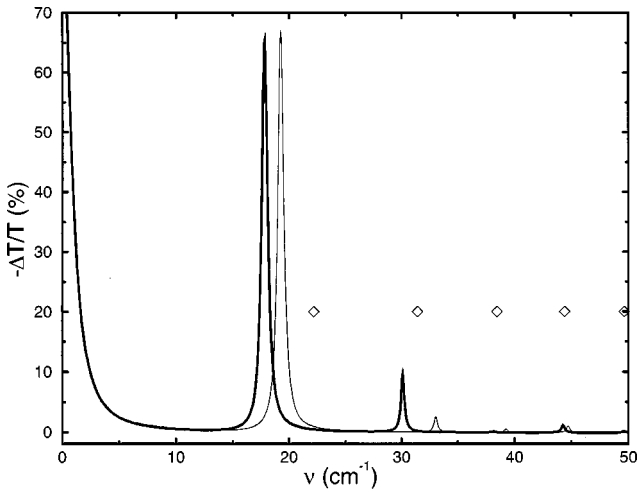

FIG. 7. Transmission spectrum of a grating and nearby 2DEG. Everything is the same as in Fig. 6 except that now $w/d=0.7$.

significantly from F_n's. For calculations we call the A_{jk} of Eq. (52) $A_{jk}^{(o)}$ and can use for them the analytic tricks in Eq. (55). Then the new

$$A_{jk}=A_{jk}^{(o)}+\frac{\tilde{\sigma}_0}{2}\sum_{n>0}\beta_n^{(j)}\beta_n^{(k)}[1/\mathcal{F}_n-1/F_n] \tag{67}$$

are readily found.

To develop a model calculation, we make the further simplification that the nearby system is a (stationary) 2D electron gas (2DEG) in the $x=h$ plane characterized by the 2D conductivity

$$\Sigma_s=i\frac{Ne^2/m^*}{\omega+i/\tau}. \tag{68}$$

The reflection amplitudes are then easily found to be

$$\mathfrak{r}_n=-1+\left(1+\frac{2\pi i}{\omega\epsilon_b}\Sigma_s G_n\right)^{-1}. \tag{69}$$

By ignoring $1/\tau$ the $\mathfrak{r}_n$ have simple poles at the frequencies

$$\omega_n^2=\frac{2\pi Ne^2}{m^*\epsilon_b}G_n. \tag{70}$$

The grating coupler will determine the extent that these modes appear in a transmission experiment. To allow for unpolarized incident light we replace the T of Eq. (2) with $\frac{1}{2}(T_{yy}+T_{zz})$, where[5]

$$T_{zz}=\left|\frac{2}{1+\sqrt{\epsilon_b}+(4\pi/c)\Sigma_s}\right|^2\sqrt{\epsilon_b}, \tag{71}$$

$$T_{yy}=\left|\frac{2}{1+\sqrt{\epsilon_b}+(4\pi/c)\Sigma+(4\pi/c)\Sigma_s}\right|^2\sqrt{\epsilon_b}, \tag{72}$$

with Σ from either Eq. (20) or Eq. (53), using $\mathcal{F}_n$'s. Typical results are shown in Figs. 6 and 7 where we have chosen for the 2DEG $N=3\times10^{11}/\mathrm{cm}^2$, $m^*/m=0.067$, and $\tau=15$ ps. The grating is described by a frequency-independent $\bar{\sigma}^{-1}=1\ \Omega/\square$ with $d=2\ \mu$m and $h/d=0.08$. We are plotting the relative change in the transmission when the 2DEG is present and absent. The structure running off-scale at low frequency is due to Σ_s alone. The modes described in Eq. (70) are responsible for the sequence of peaks at higher frequencies. The grating coupler shifts the mode locations and determines their strength in the $\Delta T/T$ spectrum in a fashion that depends on w/d. Our particular interest is in how these influences depend on the theory used for the grating. For $w/d=0.3$ in Fig. 6, Mikhailov's approximation works quite well, but for $w/d=0.7$ in Fig. 7 it leads to 10% errors in mode locations and sometimes more in mode strength. These discrepancies with respect to the full theory of Σ are much larger at fixed w/d than they were for the grating in isolation.

In summary we have shown that Mikhailov's approximate analysis for a grating coupler with the special conductivity profile of Eq. (5) can work quite well. The inconsistency of its treatment of the internal $E_\parallel$ is not a serious problem. However, the improved theory developed here avoids this inconsistency and is nearly as easy to evaluate. It should be used to ensure quantitative accuracy over the whole range of w/d.

ACKNOWLEDGMENTS

Part of the calculations were done on the Cray Research-Inc. T90 system at NPACI, San Diego, CA. We are grateful to Sergej Mikhailov for helpful correspondence.

[1] J. P. Kotthaus, in *Interfaces, Quantum Wells, and Superlattices*, edited by C. R. Leavens and R. Taylor (Plenum, New York, 1988), p. 95.
[2] D. Heitmann, in *Physics and Applications of Quantum Wells and Superlattices*, edited by K. v. Klitzing and E. E. Mendez (Plenum, New York, 1988), p. 317.
[3] For a sketch of the geometry see L. Zheng, W. L. Schaich, and A. H. MacDonald, Phys. Rev. B **41**, 8493 (1990).
[4] V. B. Shikin, T. Demel, and D. Heitmann, Zh. Éksp. Teor. Fiz. **96**, 1406 (1989) [Sov. Phys. JETP **69**, 797 (1989)].
[5] W. L. Schaich, M. R. Geller, and G. Vignale, Phys. Rev. B **53**, 13 016 (1996).
[6] T. Larson, IRE Trans. Microwave Theory Tech. **MTT-10**, 191 (1962).
[7] *Electromagnetic Theory of Gratings*, edited by R. Petit (Springer, New York, 1980).
[8] P. Sheng, R. S. Stepleman, and P. N. Sanda, Phys. Rev. B **26**, 2907 (1982).
[9] R. C. Hall and R. Mittra, IEEE Trans. Antennas Propag. **AP-33**, 1009 (1985).
[10] There is a collection of articles on grating diffraction in J. Opt. Soc. Am. A **7** (8 and 9) (1990).
[11] L. Zheng and W. L. Schaich, Phys. Rev. B **43**, 4515 (1991).
[12] C. D. Ager and H. P. Hughes, Phys. Rev. B **44**, 13 452 (1991).
[13] C. D. Ager, R. J. Wilkinson, and H. P. Hughes, J. Appl. Phys. **71**, 1322 (1992).
[14] E. G. Loewen and E. Popov, *Diffraction Gratings and Applications* (Dekker, New York, 1997).
[15] G. Wendler and T. Kraft, Physica B **271**, 33 (1999).
[16] S. A. Mikhailov, Phys. Rev. B **54**, 10 335 (1996).
[17] S. A. Mikhailov, Phys. Rev. B **54**, 14 293 (1996).
[18] S. A. Mikhailov and N. A. Savostianova, Appl. Phys. Lett. **71**, 1308 (1997).
[19] S. A. Mikhailov, Phys. Rev. B **58**, 1517 (1998).
[20] S. A. Mikhailov, Recent Res. Devel. Applied Phys. **2**, 65 (1999).
[21] J. Korringa, I. H. Lin, and R. L. Mills, Am. J. Phys. **46**, 517 (1978).
[22] A. Erdelyi, *Tables of Integral Transforms* (McGraw-Hill, New York, 1954), Vol. 2.
[23] Our choice of $y=0$ in the center of a strip makes in a uniform applied field along $\hat{y}$ that E_y, σ, and J are even in y, while E_x, $\delta\rho$, and ϕ are odd in y.
[24] A. Erdelyi, *Tables of Integral Transforms* (McGraw-Hill, New York, 1954), Vol. 1.
[25] S. Mikhailov (private communication).
[26] I. S. Gradshteyn and I. M. Ryzhik, *Table of Integrals, Series, and Products* (Academic Press, San Diego, 1981).
[27] J. Dempsey and B. I. Halperin, Phys. Rev. B **45**, 1719 (1992); **45**, 3902 (1992); **47**, 4662 (1993); **47**, 4674 (1993).
[28] E. Zaremba and H. C. Tso, Phys. Rev. B **49**, 8147 (1994); Z. L. Ye and E. Zaremba, *ibid.* **50**, 17 217 (1994).
[29] V. Shikin, Zh. Éksp. Teor. Fiz. **95**, 1513 (1989) [Sov. Phys. JETP **68**, 873 (1989)]; S. S. Nazin and V. Shikin, Fiz. Nizk. Temp. **15**, 227 (1989) [Sov. J. Low Temp. Phys. **15**, 127 (1989)]; V. Shikin, S. Nazin, D. Heitmann, and T. Demel, Phys. Rev. B **43**, 11 903 (1991); S. Nazin, K. Tevosyan, and V. Shikin, Surf. Sci. **263**, 351 (1992); V. Shikin, T. Demel, and D. Heitmann, Phys. Rev. B **46**, 3971 (1992).
[30] Compared to Ref. 5 we use w for the total strip width, set the static magnetic field to zero, and introduce an Ohmic damping into the electrons' equation of motion that leads to $\tilde{\omega}^2$.
[31] *Handbook of Mathematical Functions with Formulas, Graphs, and Mathematical Tables*, edited by M. Abramowitz and I. A. Stegun (U.S. GPO, Washington, DC, 1965).
[32] G. N. Watson, *A Treatise on the Theory of Bessel Functions* (The University Press, Cambridge, 1958), p. 404.
[33] W. H. Press, S. A. Teukolsky, W. T. Vetterling, and B. P. Flannery, *Numerical Recipes: The Art of Scientific Computing* (Cambridge University Press, New York, 1989).
[34] H. Lamb, Proc. London Math. Soc. **29**, 523 (1898).
[35] W. Schaich (unpublished).
[36] For $\overline{\sigma^{-1}}=10^4\ \Omega/\square$, all the $|E_y|$'s are roughly $0.95E_0$. There is very little current flow and screening.
[37] M. G. Moharan, E. B. Grann, D. A. Pommet, and T. K. Gaylord, J. Opt. Soc. Am. A **12**, 1068 (1995).
[38] L. Li and C. W. Haggens, J. Opt. Soc. Am. A **10**, 1184 (1993).
[39] P. Lalanne and G. M. Morris, J. Opt. Soc. Am. A **13**, 779 (1996).
[40] G. Granet and B. Guizal, J. Opt. Soc. Am. A **13**, 1019 (1996).
[41] P. Lalanne, J. Opt. Soc. Am. A **14**, 1583 (1997).
[42] L. Li, J. Opt. Soc. Am. A **13**, 1870 (1996).
[43] G. Granet, J. Opt. Soc. Am. A **16**, 2510 (1999).
[44] For an analysis of the complications caused by inhomogeneity see, W. L. Schaich, P. W. Park, and A. H. MacDonald, Phys. Rev. B **46**, 12 643 (1992).